Differential Carrier Phase GPS-Aided INS for Automotive Applications

Jay Farrell, Tony Givargis, Matthew Barth

College of Engineering, University of California, Riverside 92521

Abstract

This article describes experimental results for a real-time, carrier phase, differential Global Positioning System (GPS) aided Inertial Navigation System (INS). The implementation is the result of a study to analyze the capabilities of such a system relative to the requirements of Advanced Vehicle Control and Safety Systems (AVCSS) for intelligent transportation systems. Such navigation systems have many application possibilities (e.g., aviation and precision flight, automated mining, precision farming, dredging). The implementation achieves 100 Hz vehicle state estimates with position accuracy at the centimeter level.

1 Introduction

Automated vehicle position control systems require both a means for determining vehicle position and a means for controlling the vehicle position. A variety of reference positioning systems are reviewed in [5]. This article focuses on an integrated GPS/INS approach. The specifications for such a system are based predominantly on the needs for automobile based automated transportation systems. Previous successful vehicle control experience [10] demonstrated that a sample rate of at least 25 Hz and centimeter level position accuracy are sufficient for vehicle control under nominal operating conditions. More vehicle state information and higher sample rates would allow higher performance and would possibly enable emergency maneuvering. Navigation systems achieving these specifications have application possibilities in automated mining and dredging, aviation and precision flight, and precision farming.

This article describes the experimental results of a carrier phase differential GPS-aided INS system designed to exceed these accuracy, bandwidth, and update rate specifications. Due to space limitations, the implementation approach could not be described herein. The design is described in [5]. Previous applications have implemented pseudorange based GPS-aided INS systems (see, e.g., [9]). The main novel feature of this application is the integration of INS and *carrier phase* GPS techniques in real-time to achieve the centimeter level positioning requirement of the aided INS system. Standalone carrier phase GPS positioning has been demonstrated to achieve centimeter level accuracy [1, 3], but to the authors' knowledge, this is the first paper describing an approach that successfully demonstrates real-time, carrier phase GPS-aided inertial navigation system achieving centimeter accuracy.

This article is not attempting to show that GPS-aided INS alone is sufficient for implementation of an AVCSS. Instead, the objective of this project was to design and implement a GPS-aided INS capable of satisfying the accuracy and update rate specifications required for the AVCSS application. Based on such demonstrations, GPS-aided INS techniques can be considered along with other referencing systems if three viable independent systems are to be available for AVCSS.

2 Methodology

The navigation system developed for this project incorporates a strapdown inertial navigation system with various modes of GPS aiding. Due to space limitations, the methodology can only be summarized herein. Additional information is available in [5, 6].

The GPS-aided INS was implemented as a complementary filter [2]. The noisy inertial measurement unit (IMU) outputs are processed by the INS according to eqns. (6.51-6.53) of [6]. Since the INS is an integrative process, the output of the INS can be accurately modeled as the actual state plus a predominantly low frequency error (see Section 6.4 of [6]). The INS output is processed to provide an estimate of the GPS measurement (eqn. (5.1) of [6]). The difference between the estimated GPS output and the measured differential GPS output is a signal that contains two noise components—the predominantly low frequency INS component and the predominantly high frequency differential GPS component. The frequency content of each noise component can be accurately modeled. The objective of the state estimation design is to attenuate the GPS measurement error and provide an accurate estimate of the INS state error denoted in the following by δx. Therefore, the state estimator has a predominantly low pass characteristic. Subtracting the error estimate from the INS state, in a well designed system, produces an accurate estimate of the navigation state. The complementary filter was implemented in feedback form (i.e., the estimated INS error state was fed back to correct the INS state).

In the complementary filter approach, the INS is the primary navigation system which calculates the navigation state at the high rate at which it is used for control, guidance, and planning functions. The DGPS aiding information is used when it is available and satisfies conditions designed to verify proper sensor operation. When such aiding sensor information is not available or judged inaccurate, the INS continues its normal (unaided) operation (i.e., transformation and integration of the IMU outputs). During either aided or unaided operation, the error covariance matrices propagated within the state estimation approach predict the accuracy of the state estimates. Such measures of navigation accuracy are useful in higher level reasoning loops. The main advantages of the complementary filter approach selected for this implementation are that (1) the high rate INS navigation outputs are available without latency regardless of the availability and latency of the GPS aiding information; (2) the inputs to the Kalman filter can be accurately and properly modeled as stochastic processes, as appropriate for the technique [2]; and, (3) the computationally intensive Kalman filter covariance propagation equations can be implemented at a low update rate even though the navigation state is calculated at the desired rate of the control system.

The two basic outputs of a GPS receiver are pseudo-range and carrier phase ([6]). The implementation of this project used a

two frequency receiver. Therefore, two independent pseudo-range and carrier phase measurements were available. The measurement equation for the various observables are defined in [5] and Chapter 5 of [6]. These four observables as well as a linear combination of the phase measurements called the widelane phase [7] are used in the implementation.

A receiver in phase lock on the carrier signal is able to track the relative phase shift in the carrier between any two time instants. Therefore, although the receiver cannot directly measure the number of carrier cycles between it and a given satellite, the receiver can accurately measure the change in this number of cycles. These facts result in an *integer ambiguity* in the number of cycles of the carrier between the satellite and user antenna at an initial measurement time. Each integer ambiguity is a (usually large) unknown integer constant (barring loss of phase lock). To make use of the carrier phase observable as a range estimate, the integer ambiguity must be determined.

The interest in the carrier signal stems from the fact that the non-common mode errors are much smaller than the respective errors on the code range observables. The common-mode errors are essentially the same as those on the code range observable, except that the ionospheric error effects the measurements in opposite senses. Therefore, to take advantage of the small non-common mode phase errors, the common mode phase errors must be removed. This is accomplished through differential operation. In the differential mode of operation, the common mode errors can be reduced to produce an phase observable accurate to a few centimeters, once the integer ambiguity is determined.

How to determine the integer ambiguity for each satellite is the most critical issue that must be addressed prior to using the carrier phase measurement as an INS aiding signal. One approach is to augment one additional integer ambiguity 'state' per satellite to the error model and to let the Kalman filter estimate its value [8]. This approach has three disadvantages: (1) The integer nature of the integer ambiguity is lost, since the Kalman filter estimates the additional state as a real variable; (2) The fact that the integer ambiguity is a constant is also lost, unless the range multipath is also modeled as an augmented state. If the range multipath is not modeled, then the single augmented state (per satellite) must represent both range multipath and integer ambiguity (see Section 7.4 in [6]). This error state is neither integer nor constant. (3) The additional error states increases the computational burden of the Kalman filter. Instead, the implementation described herein used an integer ambiguity search-based approach [6, 7].

3 Error Covariance Propagation
The discrete time implementation of the Kalman filter requires a discrete time state propagation matrix ϕ and discrete time equivalent process noise covariance equation $\mathbf{Q_d}$. For this implementation, the INS error state is defined to be $\delta x = [\delta p, \delta v, \delta p, \delta x_g, \delta x_a]$ where $\delta p = [\delta n, \delta e, \delta h]^T$, $\delta v^n = [\delta v_N, \delta v_E, \delta v_D]^T$, $\delta p^n = [\delta \varepsilon_N, \delta \varepsilon_E, \delta \varepsilon_D]^T$, and $\delta x_g, \delta x_a$ are augmented gyro and accelerometer error states. The state transition matrix was calculated as

$$\phi(t_2,t_1) = \begin{bmatrix} I & F_{pv}T_2 & \frac{1}{2}F_{pv}F_{vp}T_2^2 & \frac{1}{3}F_{pv}F_{vp}F_{pg}T_2^3 & \frac{1}{2}F_{pv}F_{va}T_2^2 \\ 0 & I & F_{vp}T_2 & \frac{1}{2}F_{vp}F_{pg}T_2^2 & F_{va}T_2 \\ 0 & 0 & I & F_{pg}T_2 & 0 \\ 0 & 0 & 0 & I & 0 \\ 0 & 0 & 0 & 0 & I \end{bmatrix}.$$

where $T_2 = t_2 - t_1 = 0.2s$. By the properties of state transition matrices,

$$\phi(t_n,t_1) = \phi(t_n,t_{n-1})\phi(t_{n-1},t_1) \qquad (1)$$

which allows $\phi((k+1)T_{gps}, kT_{gps})$ to be computed between GPS measurements, where eqn. (1) is initialized with $\phi(t_1,t_1) = \mathbf{I}$. At $t = T_{gps}$, the state error covariance is propagated by

$$\mathbf{P}(T_{gps}) = \phi(T_{gps},0)\mathbf{P}(0)\phi(T_{gps},0)^T + \mathbf{Q_d}. \qquad (2)$$

The continuous time error dynamics are derived and the terms F_{vp}, F_{vv}, F_{pp}, and F_{pp} defined in Chapter 6 of [6]. In particular, the terms F_{pg}, F_{va}, and F_{vp} are time varying and significantly affect the observability of the system. They are defined using the data for the $[t_n, t_{n-1})$ interval.

The discrete time process noise covariance for the $[kT_{gps}, (k+1)T_{gps})$ interval is approximated as

$$\mathbf{Q_d}(k) = \sum_1^N \phi(t_{i+1},t_i)\mathbf{Q}(t_i)\phi(t_{i+1},t_i)^T dT_i \qquad (3)$$

where $t_1 = kT_{gps}$, $t_{N+1} = (k+1)T_{gps}$, $dT_i = t_{i+1} - t_i$ and $\sum_1^N dT_i = T_{gps}$.

4 Overall System Design
The overall design is described in the following two subsections, additional detail is contained in [5, 6].

4.1 Hardware Description
The inertial instruments consist of one three axis 2g accelerometer (manufactured by NeuwGhent Technology, Inc.), and three single-axis fiber optic gyros (Hitachi HGA-D). The 2g accelerometer range is large for the lateral and longitudinal accelerations under typical conditions, but required for the vertical acceleration due to the nominal 1g gravitational acceleration. The accelerometer is an inexpensive solid state device similar to the type of instrument expected in commercial automotive applications.

The gyros have a 10 Hz bandwidth and 60 degree per second input range. Both characteristics are reasonable for the expected application conditions. A larger bandwidth and input range may be required for emergency maneuvering. The input range must be carefully considered, as resolution and scale factor errors may increase with the input range. The major drawback of the available set of gyros was the designer limited maximum sample rate of 50 Hz via a serial port connection. Although this is five times the sensor bandwidth, it still limits the (proper) INS update rate to 50 Hz. To achieve the desired implementation rate of 100 Hz with minimal delay, each sensed gyro output was assumed constant for two 10.0 ms. sample periods. Although these instruments were not ideally matched to the application, the project budget precluded purchasing alternative instruments. Even with the sensor deficiencies, the navigation system achieved the desired accuracies and the desired update rate was demonstrated. Overcoming the sensor deficiencies will only improve the demonstrated accuracy.

For the experimental results shown herein, a compass and tilt meter manufactured by Precision Navigation were used to initialize the heading, roll, and pitch. The compass was not compensated for local magnetic fields. Even without these sensors, attitude error was rapidly (e.g., one trip around the parking lot) estimated by the Kalman filter. In a commercial application, logic to store and use the last best navigation estimates (at ignition turning off) as the initial conditions for the next run could be considered. Given that the vehicle must be driven from its initial location (e.g., a parking lot)

3661

to an automated highway, the attitude errors should be observable and hence corrected by the navigation system prior to entering the automated highway system; therefore, this sensor is not expected to be necessary in commercial applications.

The data acquisition system consists of a 100 MHz IBM 486 compatible with a National Instruments data acquisition board. The GPS hardware consisted of two Ashtech Z-12 receivers. The differential base station to rover serial port connection used a 19200 baud radio modem. The base station implementation for these experiments is described in [4] as the 'basic corrections.'

4.2 Software Description
The INS operated in the fixed tangent plane system at 100 Hz. The origin was fixed at the location of the base station antenna phase center. The INS was implemented as an interrupt driven background process to ensure the designed update rate.

GPS aiding was implemented by a standard extended Kalman filter (EKF) in feedback configuration. The EKF time propagation is defined by the ϕ and Q_d parameters defined in Subsection 3. The measurement update was implemented at a 1.0 Hz rate with scalar measurement processing using the H matrix defined in Chapter 5 of [6]. The covariance R for the each measurement update is dependent on the system mode of operation as defined in the following. Four primary modes of GPS aiding were implemented:
Mode 1. INS only: This is the default mode of operation. Since INS is implemented as a background process, it will continue to run at 100 Hz regardless of the availability of aiding information. When GPS measurements are available, the software automatically switches to Mode 2.
Mode 2. Differential Pseudo-range: This is the default start-up mode. The primary objectives of this mode are to accurately estimate the navigation state errors and to switch to the widelane phase mode. Therefore, in this mode the system begins a search and verification process for the widelane integer ambiguities using the algorithm of Section 5.7.3 of [6] with $\lambda = \lambda_w = 86.2cm$. Simultaneous with the integer ambiguity search, the Kalman filter estimates the navigation state on the basis of the differentially corrected pseudo-range measurements. In this mode, the measurement noise covariance for each measurement is set to $R = 4\ m^2$. When the integer search process successfully completes, the software automatically switches to Mode 3.
Mode 3. Differential Widelane Phase: In this mode, the software attempts to estimate and verify the L1 integer ambiguities using the algorithm of Section 5.7.3 of [6] with $\lambda = \lambda_1 = 19.0cm$. Simultaneous with this integer search, the Kalman filter estimates the navigation state errors using the differentially corrected widelane phase measurements. In this mode, the measurement noise covariance for each measurement is set to $R = 0.1^2\ m^2$. When this search process is complete, the software automatically switches to Mode 4. If widelock to at least four satellites is lost, the system automatically reverts to Mode 2.
Mode 4. Differential L1 Phase: This is the desired system operating mode. To be in this mode, the system will have estimated and verified the L1 integer ambiguities for at least four satellites. While in this mode, the Kalman filter estimates the navigation error state using the differentially corrected L1 phase measurements. The measurement noise covariance for each L1 phase measurement is set to $R = 0.01^2\ m^2$.

In modes 3 and 4, the system monitors for loss of lock for each of the 'locked' satellites. If lock is lost for a satellite, then the Kalman filter will utilize the differentially corrected pseudo-range for that satellite instead of the corresponding phase measurement. The measurement information is correctly weighted by the Kalman filter by specification of the R matrix. As long as the system has lock to at least four satellites, the system is usually able to correctly determine the integer ambiguities for 'unlocked' satellites by direct estimation ($N^{(i)} = \frac{h^{(i)}}{\lambda}x - \phi^{(i)}$) instead of search. While in Mode 4, the system will search for L2 integer ambiguities. Once estimated, the L2 phase range is used as a consistency check on the L1 and widelane phase ranges. The consistency check is that the three ranges are equal (within the limits dictated by the various noise factors) and that the integers satisfy $N_w = N_1 - N_2$.

In the Differential Pseudo-range Mode it is possible to also use the differentially corrected Doppler. This would allow on-the-fly (i.e., the vehicle could be moving) integer ambiguity resolution. The modem for this implementation could not accommodate Doppler corrections along with the L1 and L2 code and phase pseudorange corrections. Therefore, we assumed the vehicle was stopped in this mode, and synthesized a zero velocity 'measurement' with a corresponding value for the sensor uncertainty. This limitation (stationary vehicle) could be eliminated through a faster (or non-packet) modem, improved message formatting, or polynomial type correction prediction to decrease the required throughput.

The GPS receiver supplies a pulse aligned with the time of applicability of the GPS measurements. Receipt of this pulse by the INS computer causes the INS state to be saved and used for computation of the predicted GPS observables. The GPS measurements are received over the serial connection 0.4-0.6 seconds after the pulse (time of applicability). The delay is dependent on the number of satellites. Base corrections, also transmitted serially, do not arrive until approximately 0.7 seconds after the time of applicability of the GPS measurement. This left 0.3 seconds to complete the EKF computation of the navigation error state and to correct the navigation system prior to beginning the processing for the next measurement epoch.

5 Experimental: Performance Analysis
Subsection 5.1 analyzes the time from initialization to each mode of system operation. Subsections 5.2 and 5.3 describe two methods designed to test the positioning accuracy of the DGPS-aided inertial navigation system. The primary variable of interest in the analysis, due to the focus on lateral control, was the lateral position accuracy. Analysis of positioning accuracy was difficult due to the lack of independent methods to measure ground truth at the centimeter level. The methodology consists of constraining the navigation system to follow a nominal trajectory. The analysis then focuses on determining the statistics of the estimated position normal to the reference trajectory. For additional data and discussion of the analysis methods, see [5].

5.1 Time to Phase Lock Analysis
This section describes an experiment that was designed to analyze the time required for the software to achieve each mode of phase lock described in Section 4.2. For each iteration of the experiment, the navigation system software was allowed to run normally until widelock, L1 lock, and L2 lock were all achieved and verified. The time that each lock status was achieved, the number of satellites, and the estimated position were written to a file. Then a software reset re-initialized the navigation system for the next iteration. The test was performed with a known baseline separation, allowing the estimated position to be use to verified correct integer lock.

3662

	Time to Achieve Lock, s.		
	Widelock	L1 Lock	L2 Lock
Mean, 7 SV's	35.6	62.0	67.2
STD, 7 SV's	31.5	39.1	40.3
Mean, 8 SV's	40.5	60.1	65.9
STD, 8 SV's	33.9	38.5	38.6

Table 1: Statistics of the time to achieve each mode of phase lock. Time is in seconds from initial system turn on.

In the 170 iterations used to generate the following data, there were no instances of incorrect phase lock. There was one 8 satellite iteration which did not achieve lock until approximately 900 seconds. This iteration was excluded from the statistical analysis.

Table 1 presents the statistics of the total time to achieve each mode of phase lock. Total time is measured from the instant at which the software reset occurs. This time includes a ten second period during which the system is in Mode 2 while using eqn. (5.75) in [6] to initialize the widelane integers prior to the widelane integer search. The indicated lock time is the time at which the integer ambiguities have been estimated and verified.

By these statistics, widelane accuracy would be available on average after 36 seconds. L1 accuracy would be available after 62 seconds. Note that the algorithm used allows the vehicle to be in motion during the search process if differential Doppler corrections are available. Therefore, as long as the average trip to the automated roadway requires in excess of 180 seconds (i.e., mean time plus three standard deviations), phase lock would be achieved. There is still the potential for performance improvement in the area of integer search algorithms. The algorithm also works for six satellites, but does not work well for five satellites.

5.2 Table Top Testing

The experiments of this section involved two steps, both completed while operating in Mode 4. First, the platform was attached to a car and driven around the parking lot for calibration purposes. Second, the platform was transferred to a table and translated repeatedly along two of the table sides. This second step provided a set of trajectories with lateral trajectory accuracy repeatable to approximately one centimeter.

After placing the navigation platform on the table top, it was cycled between three of the table corners. Motion between the corners maintained a nominally constant heading and nominally kept one platform edge along a table edge. After moving between two points, the platform remained stationary at the destination point for approximately 10 s. During the table top portion of the experiment, INS data was recorded at 10 Hz. Following the experiment, all the stationary data (detected using a threshold of $||v|| < 0.1 \frac{m}{s}$) was separated according to which of the three corner points was closest. The mean and standard deviation of the position data for each corner was recorded, see [5]. The standard deviation of the corner data was approximately 3 cm. In two independent repetition of the experiment the maximum difference in the calculated average corner positions was 3.0 cm. The typical error was 1.0 cm. Note the calculated standard deviations correspond well with the repeatability between the two data sets. Some of the deviation in the calculated corner positions results from the experimenters having to maneuver the platform slowly near each corner to achieve the correct position and alignment.
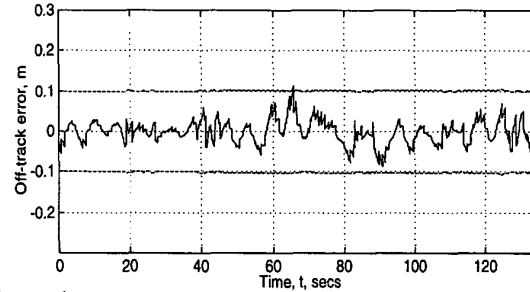

Figure 1: Table Top Navigation Test 1. Off-track Error versus Time. The dashed lines represent the standard deviation of the off-track error calculated from the Kalman filter error covariance matrices.

Figures 1 presents an example of the off-track error[1] versus time for one of the experiments. The dashed line on the figure is the navigation system estimate of the off-track error standard deviation, immediately prior to the Kalman Filter correction. For this experiment, the overall standard deviation of the off-track error data was 2.8cm. This off-track error includes the effects of erroneous motion by the experimenters and multipath. No special multipath precautions were used.

5.3 Amusement Park Ride Testing

A second set of tests was designed to test the navigation system under significant loading (i.e., accelerations and turn rates). A main difficulty was finding a test scenario allowing error calibration to the centimeter level. Ultimately, the testing of the navigation system accuracy occurred at a local amusement park (Castle Park) on the 'Wipeout' ride. The instrument platform was attached to one of the cars on the ride. Batteries, computer equipment, and modems were loaded on the car floor. The car and ride were constrained so that, nominally, the navigation system followed a circular path inclined to the surface of the earth at about fifteen degrees. The projection of this circle onto the tangent plane is an ellipse. The ride operator is only able to cycle the ride on or off. When on, the ride accelerates to a rate that would saturate the gyros. When the key is off, the ride automatically applies breaking to a stop. Therefore, for these experiments, the operator had to alternately cycle the ride off and on to keep the ride spinning, but at a reasonable rate. This cycling of the ride is expected to cause mechanical movement and vibration which will cause the actual trajectory to deviate from the nominal circle. In the results that follow, no special precautions were taken either at the base or rover to accommodate multipath effects. Multipath effects should be significant due to the large number of metal surfaces.

The navigation system position accuracy is analyzed by comparing the navigation system position estimates to a curve fit representing the nominal trajectory. Therefore, the analysis proceeds by first determining a best fit ellipse to the trajectory data and then analyzing the discrepancy of the navigation position estimates from the best fit ellipse. Photographs, figures, and a detailed description of the experimental analysis can be found in [5].

Three data sets were acquired. Two of the data sets used L1 carrier phase aiding. One of the data sets used widelane carrier phase aiding. Data corresponding to one of the L1 data sets is included. A major source of error in this experiment is mechanical motion, vibration, and flex of the ride which causes the actual path to de-

---

[1]See [5] for a detailed description of the method used to calculate off-track error and for plots of other INS variables during the experiment.
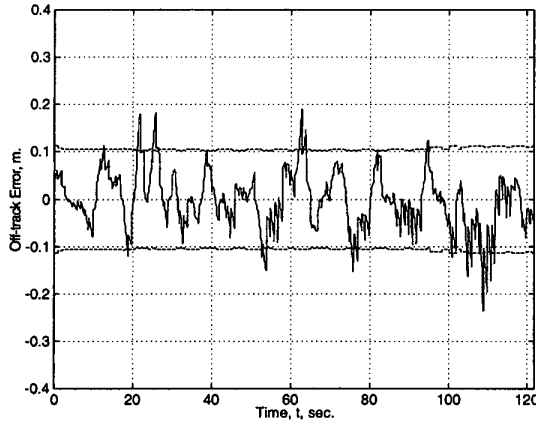
Figure 2: Amusement Park Ride L1 Test. Radius Error vs. Time.

viate from its assumed elliptic shape. Therefore, a significant (but unquantifiable) portion of the 'off trajectory error' is caused by the actual trajectory deviating from the assumed ellipse, not by navigation system error.

Figure 2 displays the off trajectory error versus time for an experiment while in L1 mode. The figure also shows the navigation system estimate of the off-track error standard deviation at a one Hz rate, calculated immediately prior to the Kalman filter measurement update. The standard deviation of the experimental off-track error for this L1 experiment was 5.98 cm. This total standard deviation would be explained by 5 cm of ride standard deviation (e.g., mechanical flex) root sum squared with the 2.5 cm of navigation system error standard deviation observed in the table top experiments. Five centimeters of mechanical motion deviation from the least squares trajectory is reasonable. The standard deviation of off-track error for the widelane experiment was 5.50 cm. The widelane GPS position error standard deviation is expected to be ≈ 5.6 times that of the L1 phase GPS error standard deviation. The fact that the errors in the two experiments are nearly identical in magnitude indicates that there is a more dominant error source such as the mechanical motion of the ride. Therefore, we conclude that the navigation system portion of the error is smaller than the 5 cm of off-track error depicted in Figure 2.

6 Conclusions and Future Research

This paper presents experimental results for a differential carrier phase GPS-aided INS that achieved the objective a 100 Hz update rate and centimeter level position accuracy. The exact position accuracy achieved is difficult to quantify due to the difficulty of obtaining a second ground truth measurement accurate to at least the centimeter level. In attaining these results, no special precautions were taken to mitigate multipath effects and no special coding (e.g., eliminating multiplication of zero matrices in the time propagation equations) was implemented. Additional efforts in algorithm design could substantially increase the INS update and GPS correction rates. Neither speedometer, odometer, nor brake pulse information was used in this implementation. Such information could be used and is available for free on many vehicles. Incorporating such signals would require extra computation for sensor calibration, but could provide both additional aiding and failure detection information.

The IMU platform for this project was crude by typical INS standards. The authors did not use special test labs or manufacturing facilities for accurate system calibration and alignment. Still,

very accurate navigation accuracy was achieved. Better accuracy should be achievable at low cost with a well designed automated manufacturing process which (1) places each instrument on the platform in a repeatable fashion; (2) performs an automated set of simple calibration procedures for each platform; and, (3) stores the calibration parameters in onboard non-volatile memory. Such a process is not unreasonable for the high volume production that could be expected in the automotive industry.

In conclusion, carrier phase DGPS-aided INS approaches provide an accurate, high rate, and reliable navigation solution. With the cost of single channel GPS hardware now below $100 (and recent revisions of the GPS signal structure) and the cost of INS sensors also decreasing, carrier phase DGPS-aided INS approaches such as that described herein may soon become available for widespread automotive, aircraft, farming, dredging, and mining applications.

7 Acknowledgments

References

[1] Blomenhofer, H., G. Hein, E. Blomenhofer, and W. Werner, "Development of a Real-Time DGPS System in the Centimeter Range," *IEEE 1994 Position, Location, and Navigation Symposium*, Las Vegas, NV, 1994, pp. 532-539.

[2] Brown, R. G., "Integrated Navigation Systems and Kalman Filtering: A Perspective," *Navigation: Journal of the Institute of Navigation*, Vol. 19 (1), Winter 1972-1973, pp. 355-362.

[3] Cannon, E. "High-Accuracy GPS Semikinematic Positioning: Modeling and Results," *Navigation: Journal of the Institute of Navigation*, Vol. 37, No. 1, Summer 1990, pp. 53-64.

[4] Farrell, J. A., and T. Givargis, "Differential GPS Reference Station Algorithm: Design and Analysis," submitted to IEEE Transactions on Control System Technology, 21 July 1998.

[5] Farrell, J. A., M. J. Barth, R. Galijan, and J. Simko, "GPS/INS Based Lateral and Longitudinal Control Demonstration: Final Report," California PATH Research Project MOU 292, UCB-ITS-PRR-98-28, September, 1997.

[6] Farrell, J. A., and M. Barth, *The Global Positioning System and Inertial Navigation*, McGraw-Hill, ISBN-0-07-022045-X, 1999.

[7] Hatch, R., "The Synergism of GPS Code and Carrier Measurements," Proc. 3rd Int. Geodetic Symposium on Sat. Doppler Pos., 1982, Las Cruces, NM.

[8] Hwang, P., "Kinematic GPS for Differential Positioning: Resolving Integer Ambiguities on the Fly," *Navigation: Journal of the Institute of Navigation*, Vol. 38 (1), Spring 1991.

[9] B. Parkinson and P. Axelrad, *Global Positioning System: Theory and Applications*, Vol. II, AIAA, 1996.

[10] H.-S. Tan, R. Rajamani, and W.-B. Zhang, "Demonstration of an Automated Highway Platoon System," *American Controls Conference*, Philadelphia, PA, 1998, pp. 1823-1827.